Heliyon 8 (2023) e12629

Contents lists available at ScienceDirect

Heliyon

journal homepage: www.cell.com/heliyon

Research article

Physicochemical properties and salinization characteristics of soils in coastal land reclamation areas: A case study of China-Singapore Tianjin Eco-City

Haixia Zhao [a,*], Binjie Gu [a], Dechao Chen [b], Jiaojiao Tang [b], Xinliang Xu [c], Zhi Qiao [d], Junqi Wang [a]

[a] Nanjing Institute of Geography and Limnology, Chinese Academy of Sciences, Nanjing 210008, China
[b] National and Local Joint Engineering Laboratory of Municipal Sewage Resource Utilization Technology, Jiangsu Key Laboratory of Environmental Science and Engineering, School of Environmental Science and Engineering, Suzhou University of Science and Technology, Suzhou 215009, China
[c] State Key Laboratory of Resources and Environmental Information Systems, Institute of Geographical Sciences and Natural Resources Research, Chinese Academy of Sciences, Beijing 100101, China
[d] School of Environmental Science and Engineering, Tianjin University, Tianjin 300072, China

ARTICLE INFO

Keywords:
Soil salinization
Salinization properties
Spatial interpolation
Principal component analysis
Tianjin City

ABSTRACT

Land salinization is a global environmental problem, and how to manage saline soils and promote healthy ecosystems has become a major challenge. China-Singapore Tianjin Eco-City is located in coastal land reclamation areas, so salinization is severe in this region. In this study, geostatistical methods, the ordinary kriging method, and principal component analysis were used. Vertical sampling was performed over three layers (0–20 cm, 20–40 cm, and 40–60 cm) at 184 locations within the study area to produce a total of 542 soil samples. It was found that areas with soluble salt contents greater than 3000 mg/kg account for over 90% of the study area, and high soluble salt content in surface layer soils is the dominant factor in soil salinization. Na^+, Cl^-, and SO_4^{2-} are the primary control factors that determine the coefficient of variation of the soils' soluble salt content. Total salinity and Na^+, Cl^-, SO_4^{2-}, K^+, and Mg^{2+} reflect on the salinization of the soils, while effective phosphorus, available potassium, and soil organic carbon reflect on the state of soil nutrition. Based on our results, we proposed site-specific and scientific soil remediation and greening measures.

1. Introduction

Soil salinization is an environmental hazard caused by natural factors or human activities, and more than 831 million hm^2 of soil is threatened by salinization worldwide (Dehaan and Taylor, 2002; Li et al., 2014, 2018). Studies have shown that by 2050, more than 50% of the world's cropland could be saline, most of it in arid and semi-arid regions (Flowers and Flowers, 2005; Wang et al., 2008). Soil salinization is a land degradation process that leads to excessive accumulation of soluble salts in the soil (Hassani et al., 2021). Soluble salts from natural processes come mainly from rainfall, aeolian processes, weathering of parent rocks or transport of saline sediments by streams or shallow groundwater (Rengasamy, 2006; Daliakopoulos et al., 2016). However, human activities also lead to soil salinization from time to time. Examples include irrigation with water containing too much salt, groundwater rise due to improper water management, seawater intrusion into coastal aquifers, and overuse of chemical fertilizers (Pannell and Ewing, 2006; Daliakopoulos et al., 2016). Due to various factors, soil salinization is expanding continuously around the world (Schofield and Kirkby, 2003). To this date, only limited progress has been made in the control of secondary salinization and the remediation of naturally saline soils.

Soil salinization has led to a global expansion of saline-alkali soils. Saline-alkali soils is an umbrella term for soils that are affected by saline and alkaline components within the soil body (this includes saline soils, alkali soils and other soils that display varying degrees of salinization and alkalinization) (Bai et al., 2018; Ju et al., 2018). Salinization generally refers to the accumulation of neutral or near-neutral salts like NaCl, $CaCl_2$, Na_2SO_4 and $MgSO_4$ in the surface layer and soil body, which cause the soil to exhibit neutral or alkaline reactions (Herbert et al., 2015; Kaushal et al., 2018a, 2018b; Li et al., 2018). Alkalinization refers to the

* Corresponding author.
E-mail address: hxzhao@niglas.ac.cn (H. Zhao).

https://doi.org/10.1016/j.heliyon.2022.e12629
Received 5 September 2022; Received in revised form 3 December 2022; Accepted 19 December 2022

entry of a certain amount of exchangeable sodium (Na^+) into the soil (Wang et al., 2009). This leads to high exchangeable sodium contents in soil colloids, high alkalinity in the soil solution, and degradation of the soils' physicochemical properties (Ouimet et al., 2008). Most studies around the world about the formative mechanisms of saline-alkali soils have focused on the patterns of water and salt transport in soils (Heng et al., 2018; Xu et al., 2019; Yuan et al., 2019). The control of water evaporation from soil based on the characteristics of water and salt transport could effectively reduce the accumulation of salts on soil surfaces, thus helping to remediate saline-alkali soils (Wang et al., 2017). Soil physicochemical properties show great spatial variability, indicating that soil management can take into account the spatial heterogeneity of saline soil types (Wang et al., 2020).

Almost 100 cities in China are located in areas that contain saline-alkali soils, and almost 33.3 million hm^2 of agricultural land (for 4.88% of all arable land in China) has been abandoned or become less productive due to soil salinization (Xie et al., 2019). The Huang-Huai-Hai Plain is an important grain producing area in China, but soil salinity has been an environmental problem in this region since the 1980s, and the Chinese government has made great efforts to improve the soil environment (Zhang et al., 2020). And the Huang-Huai-Hai Plain includes one of China's important urban agglomerations, the Beijing-Tianjin-Hebei region. It is an important economic growth pole in China with active economic activities. To relieve the pressure of land shortage, large areas of land have been reclaimed around Bohai Bay (Zhu et al., 2019). Tianjin Binhai New Area is an important area of land reclamation in the region, and one study found that 34.44% of it had already started to be exploited in 2015 (Chu et al., 2019).

Coastal areas are not only the most naturally active, ecosystem-rich and resource-rich areas on the earth's surface, but also the most densely populated and economically developed areas for human activities (Jiang et al., 2021). Driven by the growing demand for land resources, more and more reclamation activities are taking place in coastal areas around the world, and human activities have become one of the major drivers of shoreline change (Rosenberger et al., 2008). Although land reclamation has brought great benefits to society, it has also brought serious environmental problems (Chen et al., 2017). China's coastal wetlands are under tremendous pressure and face great potential risks (Tian et al., 2016). Satisfactory management of coastal land reclamation is a challenge for the Chinese government (He et al., 2012). As China-Singapore Tianjin Eco-City is located in a marine regression zone and reclaimed lands, its soils and groundwater naturally contain high levels of salt, and secondary salinization is severe in this region (Caprotti, 2014). In this work, we elucidated the physiochemical properties of saline-alkali soils in Tianjin Eco-City and its spatial distribution by determining the geochemical background values of soils in this region. Furthermore, a detailed analysis was carried out on the salinization properties of these soils. The results of this study provide a theoretical basis that will inform decisions about soil salinity management, greening efforts, and similar development/use of soils in reclaimed areas.

2. Materials and methods

2.1. Study area

China-Singapore Tianjin Eco-City is located in the Coastal Leisure & Tourism Zone of Binhai district in Tianjin City. Its distance to the coastline is less than 1 km, and its total area is approximately 30 km^2. The study area has a temperate continental monsoon climate and also exhibits some of the features of oceanic climates. The average annual rainfall in this area is 602.9 mm. The weather is usually dry and windy in spring, very wet and humid in summer, and dry and cold in winter. The study area has a flat and low-lying terrain formed by marine sedimentation. The groundwater in this area is usually located around 90 cm below the surface. It is brackish, and has pH values greater than 8.5. Its mineralization is generally greater than 10 g/L. The shallow ground layers are composed of artificial fill, littoral strata, interbedded terrestrial-marine strata and lacustrine strata, and these layers form coastal saline soils through rainwater percolation and microbial actions. The salt contents of the soils' surface layers are very high (Yee et al., 2012; Caprotti, 2014; Flynn et al., 2016; Zhan et al., 2018; Liu et al., 2019). It aims at ecological restoration and protection, building a symbiotic ecosystem of natural and artificial environment, and realizing the harmonious coexistence of man and nature. However, soil salinization has become a major problem plaguing this region.

2.2. Method

2.2.1. Sample acquisition and analysis

The study area was divided into four zones: the northwestern (NW), eastern (E), southern (S), and western (W) sampling areas, according to background surveys on the study area's topography, soils, and vegetation. 184 sampling points were set up in these areas, with three sampling strata along the vertical direction (0–20 cm, the "surface layer", 20–40 cm, the "middle layer", and 40–60 cm, the "deep layer"); a total of 542 samples were collected. The natural landscapes of the sampling points are consistent with the requirements of studies about the background values of soil environments: we selected locations with distinct soil-type characteristics, flat and stable terrain, and healthy vegetation. The sampling points were selected in strata that show well-developed soil profiles, distinct stratification, and an absence of intrusive bodies. Sampling points were not set up in locations with subordinate landscape features like foothills and swamps, or areas that are severely affected by human activities like residential areas, fields, or dung pits. Three to four sub-samples were collected in locations that show large variations in their surrounding soils and vegetation. After these samples were mixed evenly, they were quartered into approximately 500 g samples and stored in ziplock bags to form representative samples.

Analytical measurements were performed on the soil samples by applying national/industry standard methods (Kennedy and Papendick, 1995). According to the literature and relevant national standards for soil environment in China, the 13 physicochemical soil indices were measured, including HCO_3^-, CO_3^{2-}, Ca^{2+}, Mg^{2+}, K^+, Na^+, Cl^- and SO_4^{2-} contents, soil organic carbon (SOC), effective phosphorus, available potassium, pH, and soluble salt content (Wang et al., 2019). All samples were dried in the shade, grinded, and screened prior to laboratory testing. More specifically, the measurement of soil HCO_3^- and CO_3^{2-} contents was performed by double indicator titration; the volumetric method was employed to determine soil Ca^{2+} and Mg^{2+} contents; soil K^+ and Na^+ contents were assessed by flame photometry; soil Cl^- content was determined by titration with silver nitrate; soil SO_4^{2-} was calculated by the volumetric method. SOC was measured by the volumetric potassium dichromate method. Effective phosphorus was determined by the sodium bicarbonate method. Available potassium was measured by the ammonium acetate – flame photometry method. Soil pH was assessed by the potentiometric method. Finally, the total soluble salt content of the soils was determined by the gravimetric method.

2.2.2. Quality validation for the number of sampling points

Samples are randomly sampled individuals from some larger body, and differences are always present between these individuals. These samples and the overall body therefore have a "kinship" that allows the sample to represent the overall body, albeit with some differences; the smaller this difference, the more representative a sample. To achieve a high level of representativeness in the acquired samples, all subjective factors must be avoided. This is so that all of the individuals that make up the overall body are equally likely to be selected as samples. In other words, the individuals that make up the samples must be randomly selected from the overall body.

Eq. (1) gives the number of samples based on the coefficient of variation (Cv) and relative standard deviation (m) (Calzada and Scariano, 2013; Tran et al., 2019):

$$N = \frac{(t^2 Cv^2)}{m^2} \quad (1)$$

In this equation, N is the number of samples; t is the t-value that corresponds to a selected level of confidence with a certain degree of freedom; Cv is the coefficient of variation (in units of %); m is the acceptable relative standard deviation (in units of %), which is usually 30% in soil environment monitoring studies.

Since the value of t satisfies a t-distribution, the t-distribution probability, p, of a certain t-value can be calculated using the *TDIST* function Darabi-Golestan and Hezarkhani (2019):

$$TDIST\ (t, df, tails) \quad (2)$$

In this equation, t is the numerical value whose distribution is being calculated, and it is obtained from the experimental data using Eq. (1). df (degrees_freedom) is an integer that represents the degrees of freedom; in the t-distribution of a single variable, $df = N - 1$. *Tails* is the number of tails (one-tailed or two-tailed) of the returned distribution function; if $tails = 1$, the *TDIST* function returns a one-tailed distribution, and if $tails = 2$, the *TDIST* function returns a two-tailed distribution.

2.2.3. Method for spatial interpolation

As the spatial distribution of soil salinity is highly complex, it is imperative to optimize the configuration of soil sampling points to improve sampling efficiency and accuracy (Zou et al., 2013). However, it is often impossible to meet the requirements for analyzing a continuous soil surface in some areas of study, using only a limited number of soil sampling points. Therefore, the selection of a method for spatial simulation and prediction is a necessary step for predicting the spatial distribution of soil properties in an unknown area. In geostatistics, kriging has been shown to be a highly effective method for interpolating the spatial differentiation of soil properties and predicting soil distribution patterns. Kriging is a method based on variogram theory that returns the Best Linear Unbiased Prediction (BLUP) of intermediate values and comprehensively accounts for the spatial trends, correlations and randomness of regional variables (Kleijnen, 2009, 2017; Echard et al., 2013). In this study, spatial interpolation was performed using ordinary kriging with a spherical variogram model, which has a spatial resolution of 16 m.

2.2.4. Principal component analysis

It is possible for many variables to simultaneously correlate with a single observable feature. This makes it difficult to find representative variables that are mutually independent, thus hindering further research on the subject. Principal component analysis (PCA) was used to address this issue. PCA enables the identification of the characteristic factors that are responsible for soil salinization in the study area, and the conversion of multiple correlated variables into mutually independent combined variables, while preserving most of the information contained by the data (Bro and Smilde, 2014; Jolliffe and Cadima, 2016). These combined variables (principal components) may then be used as indices to assess the salinity of the study area. The averages, standard deviations and Cv values of the soils' physicochemical indices were analysed using the SPSS 17.0 program to extract the principal components of the soils' salinization properties.

3. Results

3.1. Validation of sampling point quality

Total soluble salt content is the primary control factor for soil quality in the study area. The Cv values of the total soluble salt contents in the 0–20 cm, 20–40 cm and 40–60 cm layers in each region were substituted into Eq. (1) to derive their t-values, which were then compared to the t-95% and t-90% values obtained from look-up tables. The TDIST function was then used to calculate p-values to evaluate the statistical significance of the data (Table 1).

In Table 1, it is shown that the t-values of the total salt contents of all zones and strata (except for Zone E) are greater or much greater than t-95%; the t-value of the surface layer in Zone E is slightly lower than t-95% but still much greater than t-90%. Except for the surface layer of Zone E, the p-values calculated from the t-values and degrees of freedom are either significant or extremely significant. Hence, it may be concluded that the total soluble salt content data in each zone and stratum reliably represent all information in their corresponding zones and strata, within the 95% confidence interval.

3.2. Spatial differentiation of the soil physicochemical properties

3.2.1. Soluble salt content

Soil salinization is severe throughout Tianjin Eco-City, and soil salinization is present in varying degrees throughout the depth of its soil profiles (Figure 1). Saline soil (soils with soluble salt contents greater than 6000 mg/kg) are widely distributed in each zone, and the area covered by saline soils accounts for more than 50% of the total area at each depth (51.1% in the surface layer (Figure 1a), 50.5% in the middle layer (Figure 1b), 68.1% in the deep layer (Figure 1c)). The north-eastern section of Zone NW only exhibits a light level of soil salinization (soluble salt contents between 1000 mg/kg and 2000 mg/kg), and these lightly salinized soils account for less than 7.5% of the study area.

Due to the effects of soil depth, soluble salt content increases with soil depth in Zone S and Zone W. In Zone E, the spatial differentiation in soluble salt contents decreases with increasing soil depth, causing the distribution of salt content to gradually become more uniform at deeper levels. In Zone NW, the distribution of soluble salt content across this region is not significantly affected by soil depth. It is thus shown that the change in soluble salt content with soil depth varies from one zone to another. This could be caused by local hydrogeological and topographical conditions and human activities.

3.2.2. Soil pH

Most of Tianjin Eco-City is covered by alkaline soils (Figure 2). Alkaline soils (pH > 8.5) are mainly found in Zone NW, the southern and northern parts of Zone E, Zone S and the central and northern parts of Zone W. The area covered by alkaline soils accounts for 16.7% of the surface layer (Figure 2a), 21.7% of the middle layer (Figure 2b) and 15.0% of the deep layer (Figure 2c).

The effects of soil depth on the distribution of soil pH are as follows: as soil depth increases, the distribution of alkaline soils shifts northwards in Zone E, southwards in Zone W, and gradually expands in Zone NW.

3.2.3. Na^+ and K^+ contents

The soils of Tianjin Eco-City generally contain high Na^+ and K^+ contents (Figure 3). The regions with high K^+ and Na^+ contents (Na^+ and K^+ contents greater than 2000 mg/kg) are the northern part of Zone E, the southern part of Zone S, and the central and southern parts of Zone W. Soils with high K^+ and Na^+ contents account for 39.7%, 41.7% and 55.8% of the area of these regions in the surface, middle and deep layers, respectively (Fig. 3a-c). The vegetation in these areas is therefore significantly affected by salt stress. The soils with low K^+ and Na^+ contents (<1000 mg/kg) are mainly located in the north-eastern part of Zone NW, and the area covered by these soils' accounts for no more than 13% of the study area.

Na^+ and K^+ content is affected to some extent by soil depth. In Zones S and W, Na+ and K^+ content generally rise with increasing soil depth. In Zone E, the spatial differentiation of K^+ and Na^+ content decreases with increasing soil depth. There is a region on the northern side of Zone E that contains extremely high levels of Na^+ and K^+ (>4000 mg/kg) in the surface layer, but the Na^+ and K^+ content gradually dissipate with increasing soil depth. The effects of soil depth on the distribution of Na^+ and K^+ content in Zone NW is insignificant. The vertical and horizontal distribution of the soils' Na^+ and K^+ contents are correlated to some extent with their soluble salt content.

Table 1. Quality validation for the number of sampling points that were set up for total soluble salt content in each region.

Zone	Layer	*Cv*	N	df	t-calculated	t-95% CI on Corresponding df	t-90% CI on Corresponding df	p	Sig.
NW	Surface	1.37	70	69	1.832	1.671	1.296	0.036	*
	Middle	0.98	70	69	2.561	1.671	1.296	0.006	**
	Deep	0.88	70	69	2.852	1.671	1.296	0.003	**
W	Surface	1.15	44	43	1.730	1.684	1.303	0.045	*
	Middle	0.82	44	43	2.427	1.684	1.303	0.010	**
	Deep	0.70	44	43	2.843	1.684	1.303	0.003	**
E	Surface	1.18	43	42	1.667	1.684	1.303	0.051	.
	Middle	0.72	43	42	2.732	1.684	1.303	0.005	**
	Deep	0.70	43	42	2.810	1.684	1.303	0.004	**
S	Surface	0.88	27	26	1.771	1.706	1.315	0.044	*
	Middle	0.55	27	26	2.834	1.706	1.315	0.004	**
	Deep	0.47	27	26	3.317	1.706	1.315	0.001	***

Note: Sig. codes: 0 '***' 0.001 '**' 0.01 '*' 0.05'.'

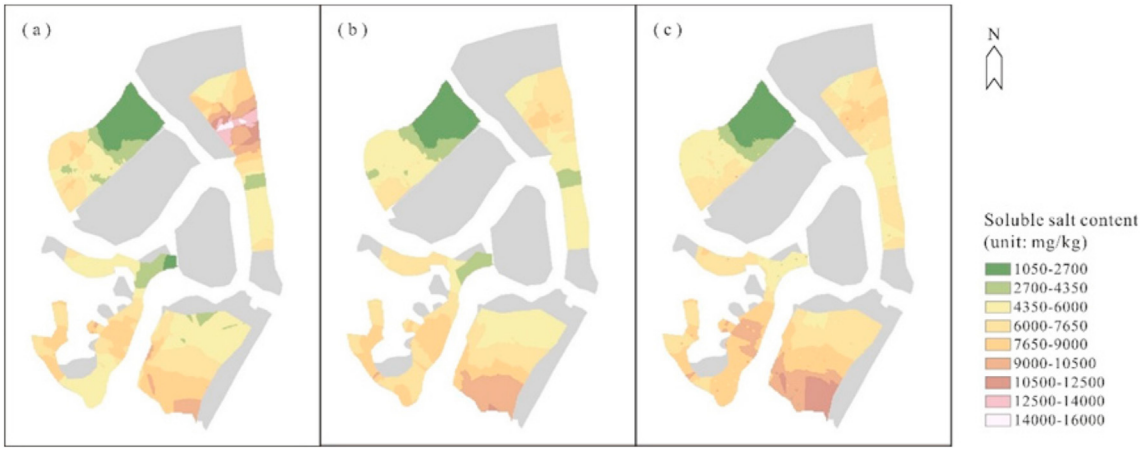

Figure 1. Spatial distribution pattern of the soils' soluble salt content (a) surface layer (b) middle layer (c) deep layer.

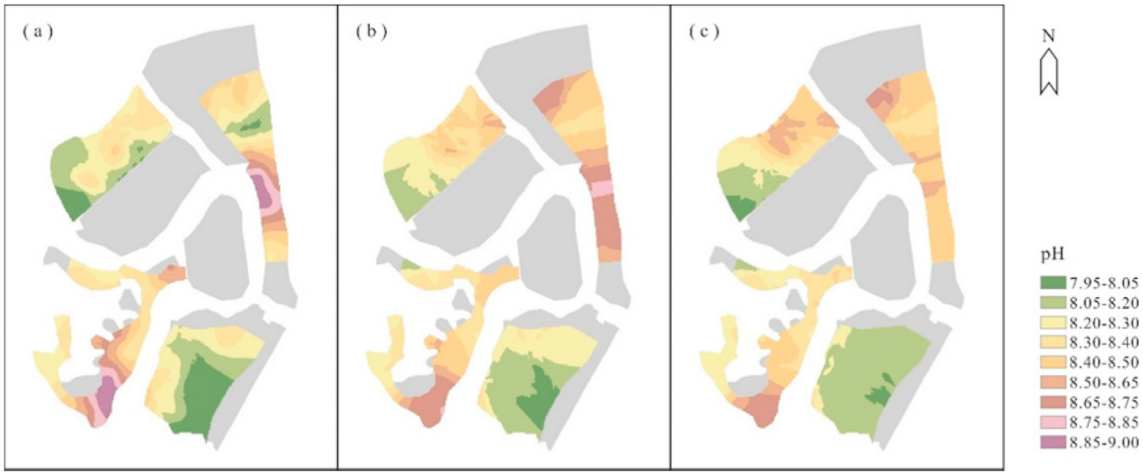

Figure 2. Spatial distribution pattern of the soils' pH content (a) surface layer (b) middle layer (c) deep layer.

3.2.4. Cl^- content

The Cl^- content in the soils of Tianjin Eco-City is generally quite high (Figure 4). The areas with high levels of Cl^- content (Cl^- content greater than 2000 mg/kg) are the southwestern part of Zone NW, Zone E, the central and southern parts of Zone S, and Zone W. These high Cl^- content areas cover over 60% of the land in these zones (70.0% of the surface layer (Figure 4a), 67.2% of the middle layer (Figure 4b) and 80.3% of the deep layer (Figure 4c)). The low Cl^- content area (<1000 mg/kg) is mainly located in the northeastern part of Zone NW, and the low Cl^- areas accounts for no more than 10% of the study area. The distribution of Cl^- content in the soils is strongly correlated with the distribution of Na^+ and K^+.

In Zone S, there is a significant positive correlation between the soils' Cl^- content and soil depth. Cl^- content and heterogeneity of Cl^- content

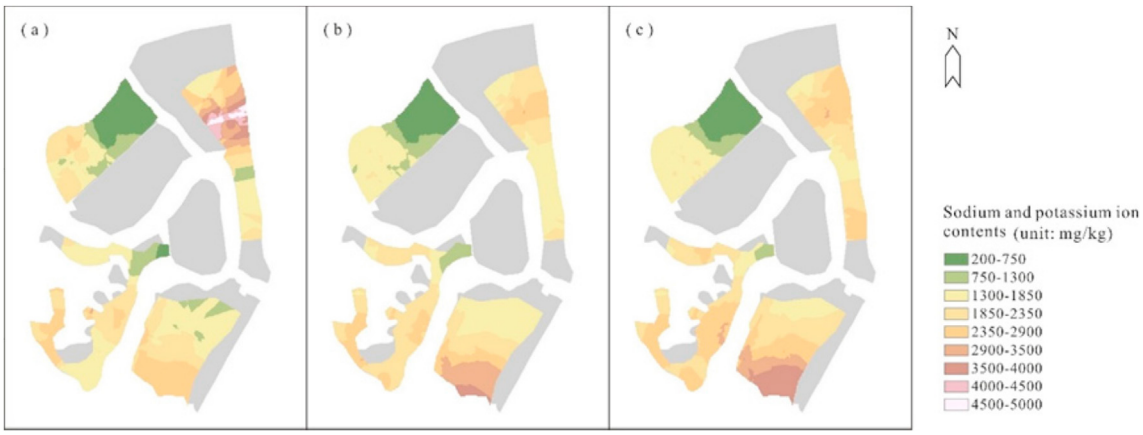

Figure 3. Spatial distribution pattern of the soils' Na^+ and K^+ content (a) surface layer (b) middle layer (c) deep layer.

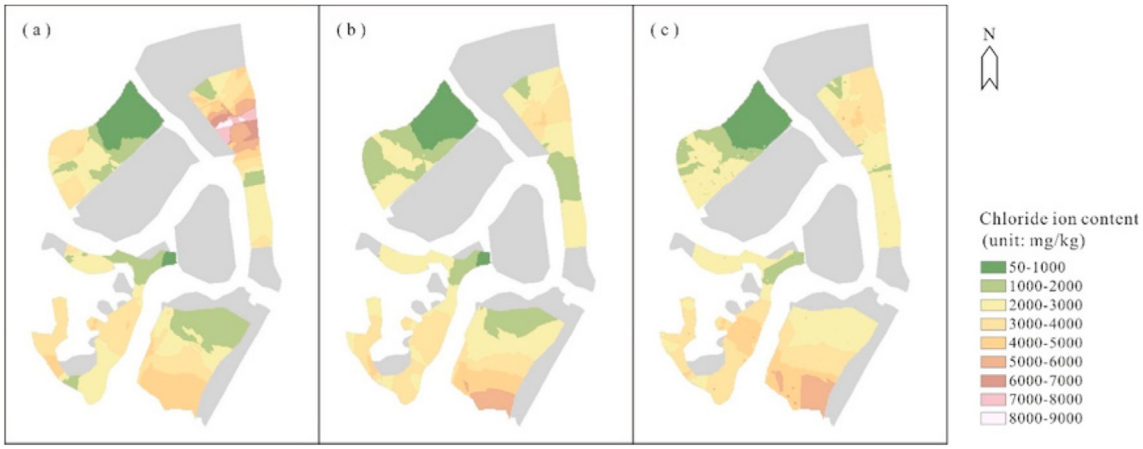

Figure 4. Spatial distribution pattern of the soils' Cl^- content (a) surface layer (b) middle layer (c) deep layer.

decreased with increasing soil depth in Zone E; an area in the northern part of this zone has extremely high Cl^- content (>6000 mg/kg), which gradually dissipates as soil depth increases. The distribution of Cl^- content in Zone NW and Zone W does not vary significantly with soil depth. In the southwestern part of Zone NW, Cl^- content decreases slightly from the surface layer to the middle layer.

3.2.5. *Effective phosphorus content*

The effective phosphorus contents of the soils in Tianjin Eco-City largely vary between the "lower-middle" and "high" levels (10–40 mg/kg) of the second Chinese soil census's soil nutrient classification standard (Figure 5). The regions with high levels of effective phosphorus (20–40 mg/kg) are mainly located in the northern, western and southern parts of Zone NW, the northern part of Zone S, and Zone W. In these regions, the area occupied by soils with high levels of effective phosphorus account for 82.4% of the surface layer (Figure 5a), 56.4% of the middle layer (Figure 5b) and 43.7% of the deep layer (Figure 5c).

The vertical distribution of the soils' effective phosphorus is a manifestation of the tendency for soil nutrients to aggregate on the surface. The horizontal area covered by high effective phosphorus soil

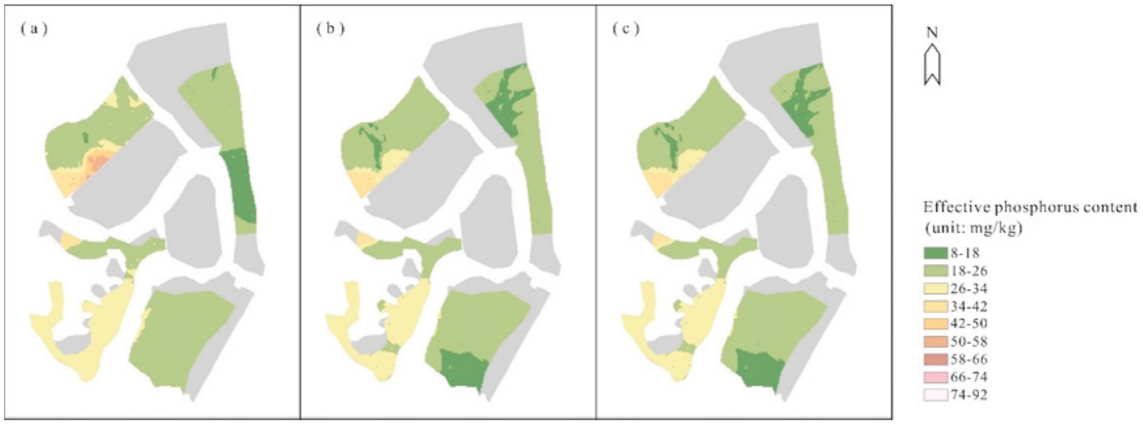

Figure 5. Spatial distribution pattern of the soils' effective phosphorus content (a) surface layer (b) middle layer (c) deep layer.

gradually shrinks with increasing soil depth. In the southeastern part of Zone NW, effective phosphorus is almost completely exhausted in the soils' middle and deep layers, even when the surface layer contains an extremely large amount of effective phosphorus (>40 mg/kg).

3.2.6. Soil available potassium

The soils of Tianjin Eco-City contain extremely high levels of available potassium, and the available potassium content of these soils generally fall in the "extremely high" level of the second national soil census's soil nutrient classification standard (>200 mg/kg) (Figure 6).

The vertical distribution of soil available potassium reflects on the tendency of soil nutrients to aggregate on the surface. The area covered by soils with high amounts of available potassium is smaller in the middle layer than in the surface layer (Fig. 6a,b). However, this area does not change significantly between the middle and deep layers (Fig. 6b,c).

3.3. Principal component analysis of the soils' salinization properties

PCA was performed on all of the measured indices of Zone NW's samples and two principal components were extracted from this process (Figure 7a). The first principal component reflects 51.4% of all information contained in the data. The total salinity, Na^+, Cl^-, SO_4^{2-}, K^+, and Mg^{2+} indices have very strong negative loadings on the first principal component, whereas pH, CO_3^{2-}, and HCO_3^- have positive loadings on this component. The first principal component may therefore be treated as a combined index that reflects the overall state of soil salinization. The second principal component accounts for 17.8% of all variances in the data. The effective phosphorus, available potassium, and SOC indices have negative loadings on the second principal component. The second principal component may therefore be treated as a combined index that reflects the state of soil nutrition. Ca^{2+} has a similar negative loading on both principal components; this indicates that Ca^{2+} is a salinization factor and a nutrient factor, and these loadings could be related to the carbon cycle between calcium carbonate and organic carbon. The total soluble salt content, Na^+, Cl^-, and pH indices have varying levels of positive loading on the second principal component. This is the exact opposite of the effective phosphorus, available potassium, and SOC indices, which are indices that generally reflect on soil fertility. Therefore, total soluble salt content, Na^+, Cl^-, and pH are the key control factors that restrict vegetation growth and the accumulation of soil fertility in Zone NW. The relative importance of these factors is as follows: $Na^+ > Cl^- >$ total soluble salt content $>$ pH.

Two principal components were obtained by performing PCA on all of the measured indices of Zone W's samples (Figure 7b). The first principal component reflects 51.9% of all information in the data. The total salinity, Na^+, Cl^-, SO_4^{2-}, K^+, and Mg^{2+} indices have very strong negative loadings on the first principal component, whereas the pH, CO_3^{2-}, and HCO_3^- indices have positive loadings on this component. The first principal component is therefore a combined index that focuses on the overall state of soil salinization. The second principal component reflects 15.9% of all data variances, and the effective phosphorus, available potassium, and SOC indices have negative loadings on this component. The second principal component is therefore a combined index that reflects the state of soil nutrition. Ca^{2+} has similar negative loadings on both principal components, which indicates that it is both a soil salinization factor and soil nutrient factor; this could be related to the carbon cycle between calcium carbonate and organic carbon. The total soluble salt content, Na^+, Cl^-, and pH indices have different levels of positive loading on the second principal component, which is the exact opposite of the effective phosphorus, available potassium and organic carbon indices. This indicates that total soluble salt content, Na^+, Cl^-, and pH are key controlling factors that limit vegetation growth and the accumulation of soil fertility in Zone NW. The relative importance of these factors is as follows: pH $> CO_3^{2-} > Na^+ > Cl^-$ $>$ total soluble salt content.

PCA was performed on all of the measured indices of Zone E's samples and two principal components were extracted from this process (Figure 7c). The first principal component reflects 58.4% of all information in the data. The total salinity, Na^+, Cl^-, SO_4^{2-}, K^+, Mg^{2+}, and Ca^{2+} indices have very strong negative loadings on the first principal component, whereas the pH, CO_3^{2-}, and HCO_3^- indices have positive loadings on this component. Therefore, the first principal component is a combined index reflecting the soil salinization's overall state. The second principal component accounts for 13.7% of all data variances, and the effective phosphorus, available potassium, and organic carbon indices all have negative loadings on this component. Therefore, the second principal component is a combined index that measures the state of soil nutrition. The main factors of soil salinization and soil nutrition are orthogonally related to each other; in other words, the effective phosphorus, available potassium, and SOC soil nutrition indices are not affected by the first principal component (the soil salinization principal component).

Two principal components were extracted from the PCA on all of the measured indices of Zone S's samples (Figure 7d). The first principal component reflects 55.9% of all information in the data. The total salinity, Na^+, Cl^-, SO_4^{2-}, K^+, Mg^{2+}, and Ca^{2+} indices have very strong negative loadings on the first principal component, whereas the pH, CO_3^{2-}, and HCO_3^- indices have positive loadings on this component. Therefore, the first principal component is a combined index that reflects the overall state of soil salinization. The second principal component accounts for 16.8% of all data variances, and the effective phosphorus, available potassium, and SOC indices have negative loadings on this component. Therefore, the second principal component is a combined index that assesses the state of soil nutrition.

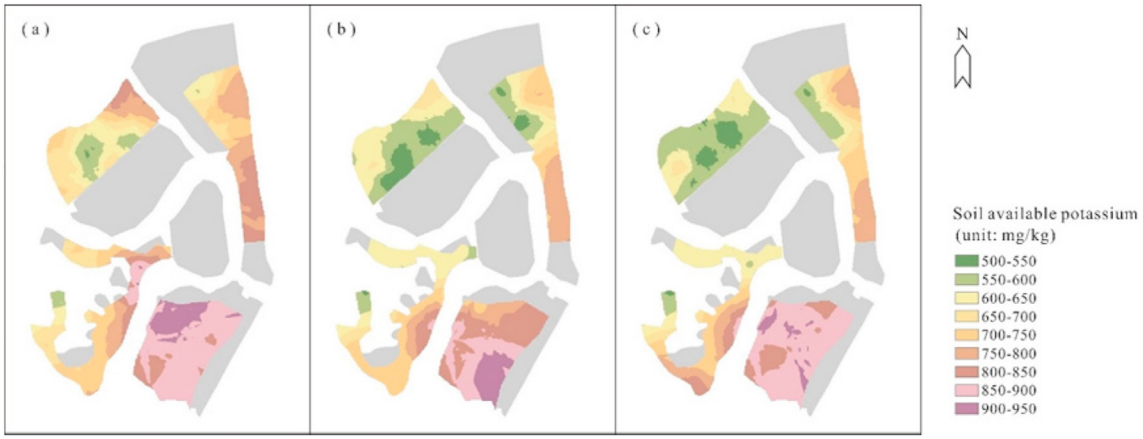

Figure 6. Spatial distribution pattern of the soils' available potassium content (a) surface layer (b) middle layer (c) deep layer.

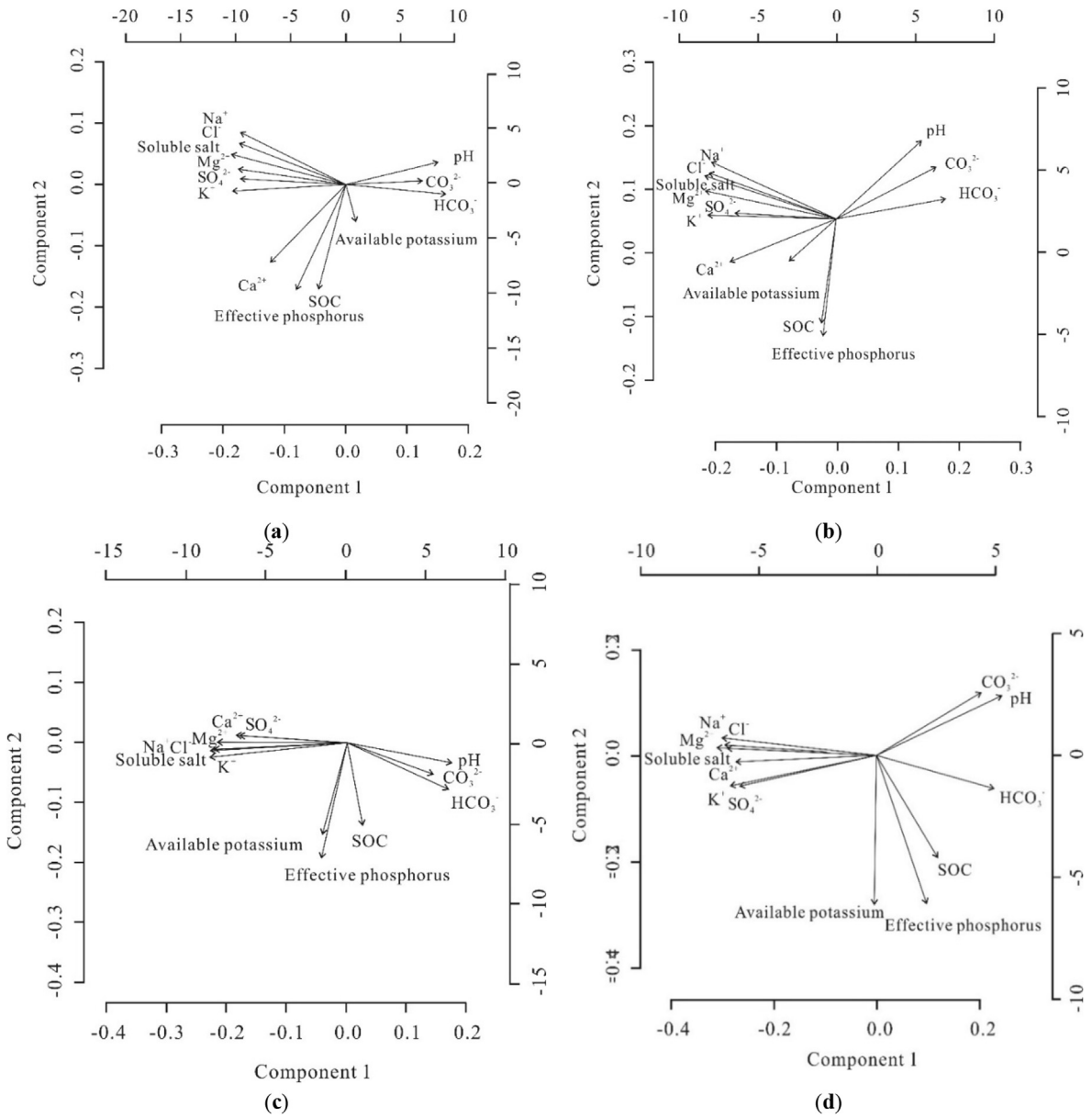

Figure 7. Principal component analysis on the soil salinization properties. (**a**) Zone NW; (**b**) Zone W; (**c**) Zone E; (**d**) Zone S.

4. Discussion

4.1. Analysis of salinization and physicochemical soil properties

Soil salinization refers to the process where soluble salts in the soil solution aggregate at the surface during drought conditions. This occurs if the water table is shallower than the critical water table depth and the groundwater has a high level of mineralization. Salinization level and salt type are the main indicators of soil's salinization properties. The degree of soil salinization generally reflects the degree of salt accumulation in saline soils or salinized soils, and this index can also be used for soil classification. The physicochemical properties, salt transport, and salt accumulation characteristics of saline/salinized soil vary for each type of salt. In addition, the degree of harm caused by soil salinization also varies with salt type. Consequently, the measures for remediating and managing soil salinization differ among different types of salt.

Statistical analysis was performed on the physicochemical soil parameters of Zones NW, W, E, and S of the study area to investigate the characteristics factors that cause soil salinization in these zones. Based on the characteristics of each zone, Zone NW has the largest number of samples and *Cv*, while Zone S has the smallest *Cv*. In terms of the pH index, Zone W has the largest proportion of high pH (pH $>$ 8.5) samples in the surface layer (43.2%), whereas Zone E has the largest proportion of high pH samples in the middle and deep layers (both 50%). The pH values of the samples in Zone S are relatively low. The main factors that control the physicochemical properties of each layer in each zone are the Na^+, Cl^-, and SO_4^{2-} contents. *Cv* gradually decreases from the surface layer to the deep layer. However, the percentage of samples with pH $>$ 8.5 does not change significantly from one layer to another.

4.2. Suggestions on preventing and managing soil salinization in coastal land reclamation areas

Based on the spatial differentiation of physicochemical properties in the saline-alkali soils of the study area and an analysis of their salinization properties, a few viable and targeted proposals are suggested in the following to prevent and manage soil salinization in coastal land reclamation areas.

In regions where soil salinization is relatively minor (salt contents lower than 3000 mg/kg), salts that are detrimental to plant growth like Na^+ and K^+ are not present in large quantities and vegetation survival rates may reach 70%–80%. It is suggested that soil monitoring works should be intensified in these areas. On this basis, organic fertilizers may be added to increase the organic matter content of the soils. This will promote the formation of soil aggregates, which will improve soil aeration and permeability. Plant communities that help to remediate soil salinization, maintain high levels of soil quality, and are aesthetically pleasing should be established by planting common green plants that are ornamentally valuable, cheap, amenable to reproductive management, and have fast-growing shallow roots, as well as certain glycophyte species.

The effects of salt stress on vegetation growth are significantly adverse in regions with soil salt contents between 3000 mg/kg and 5000 mg/kg. In this case, soil engineering measures like subsurface drainage systems, and salt barriers need to be taken in conjunction with other measures (Wang et al., 2019). A subsurface drainage system that is suited to the local geological and soil conditions can be used in combination with salt isolating and leaching techniques (e.g., salt barriers and anti-permeation barriers), rain harvesting systems and water-saving/soil salinity-controlling irrigation techniques (Xie et al., 2010; Wang et al., 2011). It is suggested that species that are able to tolerate low levels of salt content and form large amounts of organic matter to reduce cell water potential should be planted, according to the local salinization and alkalinization of the coastal region. This will form a greenbelt that is effective in remediating saline-alkali soils ().

In regions with soil salt contents between 5000 mg/kg and 10000 mg/kg, the vegetation survival rate is less than 50%. In these regions, engineering measures for the remediation of saline-alkali soils should be implemented and the monitoring of water-soil salinization should be intensified. On this basis, salinity remediating plant communities that can tolerate high salt concentrations should be established. For example, plant communities that consist of a suitable number of highly salt tolerant halophytes.

In regions with extremely severe soil salinization (soil salt contents greater than 10000 mg/kg), the effects of salt stress on vegetation growth are very significant. In these regions, engineering measures for the remediation of saline-alkali soil should be implemented, and the monitoring of soil and water salinization should be intensified. On this basis, suitable chemical measures should be implemented according to field conditions (Sadiq et al., 2007). For example, chemical remediates could be used to change the composition of cations adsorbed by soil aggregates. This would promote the formation of aggregate structures, improve soil structures, and delay the return of soil salinization. The most effective way to ensure the survival and sustainability of the plant communities is to grow salt-tolerant halophytes.

5. Conclusions

China-Singapore Tianjin Eco-City is located in the coastal land reclamation area, with high salinity content. However, as the key area of human development activities, it is particularly important to find out the physiochemical properties and spatial distribution of saline-alkali soils, analyze their formation mechanism, and further take measures of protection and improvement.

13 soil salinity and nutrition indices of a total of 542 soil samples in 184 locations were evaluated in laboratory measurements. In China-Singapore Tianjin Eco-City, areas with soluble salt contents greater than 3000 mg/kg account for over 90% of the study area, and high soluble salt content in surface layer soils is the dominant factor in soil salinization. Na^+, Cl^-, and SO_4^{2-} contents are the primary control factors that determine the coefficient of variation of the soils' soluble salt content. Total salinity and Na^+, Cl^-, SO_4^{2-}, K^+, and Mg^{2+} contents reflect on the salinization of the soils, while effective phosphorus, available potassium, and soil organic carbon (SOC) reflect on the state of soil nutrition.

Despite the spatial differentiation of physicochemical properties and salinization properties in the saline-alkali soils of China-Singapore Tianjin Eco-City, some protective measures have been suggested. These measures can provide a reference for soil remediation in coastal land reclamation areas. Future soil restoration and management should consider the heterogeneity of physicochemical properties of saline lands and their spatial distribution. We suggest that different responses should be adopted in different areas to facilitate the sustainability of soil restoration and management. In the future, these protective measures should be further validated in laboratory experiments to develop more efficient protective measures.

Declarations

Author contribution statement

Haixia Zhao: Conceived and designed the experiments; Analyzed and interpreted the data.

Binjie Gu: Analyzed and interpreted the data; Wrote the paper.

Dechao Chen: Conceived and designed the experiments; Analyzed and interpreted the data; Wrote the paper.

Jiaojiao Tang: Performed the experiments; Wrote the paper.

Xinliang Xu: Performed the experiments; Contributed reagents, materials, analysis tools or data.

Zhi Qiao: Contributed reagents, materials, analysis tools or data.

Junqi Wang: Revised the paper; Analyzed and interpreted the data.

Funding statement

This work was supported by the National Natural Science Foundation of China (41971389), Jiangsu Overseas Research & Training Program for University Prominent Young & Middle-aged Teachers and the Strategic Priority Research Program of Chinese Academy of Sciences (XDA20010302).

Data availability statement

Data included in article/supp. material/referenced in article.

Declaration of interest's statement

The authors declare no competing interests.

Additional information

No additional information is available for this paper.

References

Bai, L., Wang, C.Z., Zang, S.Y., Wu, C.S., Luo, J.M., Wu, Y.X., 2018. Mapping soil alkalinity and salinity in northern songnen plain, China with the HJ-1 hyperspectral imager data and partial least squares regression. Sensors 18, 3855.

Bro, R., Smilde, A.K., 2014. Principal component analysis. Anal. Methods 6, 2812–2831.

Calzada, M.E., Scariano, S.M., 2013. A synthetic control chart for the coefficient of variation. J. Stat. Comput. Simulat. 83, 853–867.

Caprotti, F., 2014. Critical research on eco-cities? A walk through the sino-Singapore Tianjin eco-city, China. Cities 36, 10–17.

Chen, W.G., Wang, D.C., Huang, Y., Chen, L.D., Zhang, L.H., Wei, X.W., Sang, M.Q., Wang, F.C., Liu, J.Y., Hu, B.X., 2017. Monitoring and analysis of coastal reclamation from 1995–2015 in Tianjin Binhai New area, China. Sci. Rep. 7, 3850.

Chu, J.L., Suo, A.N., Liu, B.Q., Zhao, J.H., Wang, C.Y., 2019. Remote sensing-based life cycle analysis of land reclamation processes: case study on Tianjin Binhai New area. J. Coast Res. 90, 77–85.

Daliakopoulos, I.N., Tsanis, I.K., Koutroulis, A., Kourgialas, N.N., Varouchakis, E.A., Karatzas, G.P., Ritsema, C.J., 2016. The threat of soil salinity: a European scale review. Sci. Total Environ. 573, 727–739.

Darabi-Golestan, F., Hezarkhani, A., 2019. Applied statistical functions and multivariate analysis of geochemical compositional data to evaluate mineralization in Glojeh polymetallic deposit, NW Iran. Front. Earth Sci. 13, 229–246.

Dehaan, R.L., Taylor, G.R., 2002. Field-derived spectra of salinized soils and vegetation as indicators of irrigation-induced soil salinization. Remote Sens. Environ. 80, 406–417.

Echard, B., Gayton, N., Lemaire, M., Relun, N., 2013. A combined importance sampling and kriging reliability method for small failure probabilities with time-demanding numerical models. Reliab. Eng. Syst. Saf. 111, 232–240.
Flowers, T.J., Flowers, S.A., 2005. Why does salinity pose such a difficult problem for plant breeders? Agric. Water Manag. 78, 15–24.
Flynn, A., Yu, L., Feindt, P., Chen, C., 2016. Eco-cities, governance and sustainable lifestyles: the case of the Sino-Singapore Tianjin Eco-City. Habitat Int. 53, 78–86.
Hassani, A., Azapagic, A., Shokri, N., 2021. Global predictions of primary soil salinization under changing climate in the 21st century. Nat. Commun. 12, 6663.
He, Y.Y., Xue, X.Z., Kong, H., 2012. The application of costs and benefits analysis in coastal land-reclamation. Adv. Mater. Res. 518–523, 5232–5237.
Heng, T., Liao, R.K., Wang, Z.H., Wu, W.Y., Li, W.H., Zhang, J.Z., 2018. Effects of combined drip irrigation and sub-surface pipe drainage on water and salt transport of saline-alkali soil in Xinjiang, China. J. Arid Land 10, 932–945.
Herbert, E.R., Boon, P., Burgin, A.J., Neubauer, S.C., Franklin, R.B., Ardon, M., Hopfensperger, K.N., Lamers, L.P.M., Gell, P., 2015. A global perspective on wetland salinization: ecological consequences of a growing threat to freshwater wetlands. Ecosphere 6, 206.
Jiang, S., Xu, N., Li, Z.C., Huang, C.H., 2021. Satellite derived coastal reclamation expansion in China since the 21st century. Glob. Ecol. Conserv. 30, e01797.
Jolliffe, I.T., Cadima, J., 2016. Principal component analysis: a review and recent developments. Philos. Trans. Royal Soc. A. 374, 20150202.
Ju, Z.Q., Du, Z.L., Guo, K., Liu, X.J., 2018. Irrigation with freezing saline water for 6 years alters salt ion distribution within soil aggregates. J. Soils Sediments 19, 97–105.
Kaushal, S.S., Likens, G.E., Pace, M.L., Haq, S., Wood, K.L., Galella, J.G., Morel, C., Doody, T.R., Wessel, B., Kortelainen, P., Raike, A., Skinner, V., Utz, R., Jaworski, N., 2018a. Novel 'chemical cocktails' in inland waters are a consequence of the freshwater salinization syndrome. Philos. Trans. Royal Soc. B. 374, 20180017.
Kaushal, S.S., Likens, G.E., Pace, M.L., Utz, R.M., Haq, S., Gorman, J., Grese, M., 2018b. Freshwater salinization syndrome on a continental scale. Proc. Natl. Acad. Sci. U.S.A. 115, E574–E583.
Kennedy, A.C., Papendick, R.I., 1995. Microbial characteristics of soil quality. J. Soil Water Conserv. 50, 243–248.
Kleijnen, J.P.C., 2009. Kriging metamodeling in simulation: a review. Eur. J. Oper. Res. 192, 707–716.
Kleijnen, J.P.C., 2017. Regression and Kriging metamodels with their experimental designs in simulation: a review. Eur. J. Oper. Res. 256, 1–16.
Li, J.G., Pu, L.J., Han, M.F., Zhu, M., Zhang, R.S., Xiang, Y.Z., 2014. Soil salinization research in China: advances and prospects. J. Geogr. Sci. 24, 943–960.
Li, P.Y., Qian, H., Wu, J.H., 2018. Conjunctive use of groundwater and surface water to reduce soil salinization in the Yinchuan Plain, North-West China. Int. J. Water Resour. Dev. 34, 337–353.
Liu, Y.X., Sun, X., Sun, T., Shi, X.P., Liu, J.M., 2019. Promoting green residential buildings by increasing homebuyers' willingness to pay: evidence from Sino-Singapore Tianjin Eco-city in China. J. Clean. Prod. 238, 117884.
Ouimet, R., Moore, J.D., Duchesne, L., 2008. Effects of experimental acidification and alkalinization on soil and growth and health of Acer saccharum Marsh. J. Plant Nutr. Soil Sci. 171, 858–871.
Pannell, D.J., Ewing, M.A., 2006. Managing secondary dryland salinity: options and challenges. Agric. Water Manag. 80, 41–56.
Rengasamy, P., 2006. World salinization with emphasis on Australia. J. Exp. Bot. 57, 1017–1023.
Rosenberger, E.E., Hampton, S.E., Fradkin, S.C., Kennedy, B.P., 2008. Effects of shoreline development on the nearshore environment in large deep oligotrophic lakes. Freshw. Biol. 53, 1673–1691.
Sadiq, M., Hassan, G., Mehdi, S.M., Hussain, N., Jamil, M., 2007. Amelioration of saline-sodic soils with tillage implements and sulfuric acid application. Pedosphere 17, 182–190.
Schofield, R.V., Kirkby, M.J., 2003. Application of salinization indicators and initial development of potential global soil salinization scenario under climatic change. Global Biogeochem. Cycles 17, 1078.
Tian, B., Wu, W.T., Yang, Z.Q., Zhou, Y.X., 2016. Drivers, trends, and potential impacts of long-term coastal reclamation in China from 1985 to 2010. Estuar. Coast Shelf Sci. 170, 83–90.
Tran, K.P., Nguyen, H.D., Tran, P.H., Heuchenne, C., 2019. On the performance of CUSUM control charts for monitoring the coefficient of variation with measurement errors. Int. J. Adv. Manuf. Technol. 104, 1903–1917.
Wang, L., Seki, K., Miyazaki, T., Ishihama, Y., 2009. The causes of soil alkalinization in the Songnen Plain of Northeast China. Paddy Water Environ. 7, 259–270.
Wang, J.Y., Liu, H.M., Wang, S.M., Liu, Y.X., Cheng, Z.G., Fu, G.Q., Mo, F., Xiong, Y.C., 2019. Surface mulching and a sandy soil interlayer suppress upward enrichment of salt ions in salt-contaminated field. J. Soils Sediments 19, 116–127.
Wang, J.Y., Liu, Y.X., Wang, S.M., Liu, H.M., Fu, G.Q., Xiong, Y.C., 2020. Spatial distribution of soil salinity and potential implications for soil management in the Manas River watershed, China. Soil Use Manag. 36, 93–103.
Wang, S.T., Feng, Q., Zeng, Y.P., Mao, X.X., Chen, Y.H., Xu, H., 2017. Dynamic changes in water and salinity in saline-alkali soils after simulated irrigation and leaching. PLoS One 12, e0187536.
Wang, Y.G., Xiao, D.N., Li, Y., Li, X.Y., 2008. Soil salinity evolution and its relationship with dynamics of groundwater in the oasis of inland river basins: case study from the Fubei region of Xinjiang Province, China. Environ. Monit. Assess. 140, 291–302.
Wang, Y.J., Xie, Z.K., Malhi, S.S., Vera, C.L., Zhang, Y.B., Guo, Z.H., 2011. Effects of gravel–sand mulch, plastic mulch and ridge and furrow rainfall harvesting system combinations on water use efficiency, soil temperature and watermelon yield in a semi-arid Loess Plateau of northwestern China. Agric. Water Manag. 101, 88–92.
Xie, X.F., Pu, L.J., Zhu, M., Xu, Y., Wang, X.H., 2019. Linkage between soil salinization indicators and physicochemical properties in a long-term intensive agricultural coastal reclamation area, Eastern China. J. Soils Sediments 19, 3699–3707.
Xie, Z.K., Wang, Y.J., Cheng, G.D., Malhi, S.S., Vera, C.L., Guo, Z.H., Zhang, Y., 2010. Particle-size effects on soil temperature, evaporation, water use efficiency and watermelon yield in fields mulched with gravel and sand in semi-arid Loess Plateau of northwest China. Agric. Water Manag. 97, 917–923.
Xu, C.D., Tian, J.J., Wang, G.X., Nie, J.K., Zhang, H.Y., 2019. Dynamic simulation of soil salt transport in arid irrigation areas under the HYDRUS-2D-Based rotation irrigation mode. Water Resour. Manag. 33, 3499–3512.
Yee, T.W., Lawson, C.R., Wang, Z.Y., Ding, L., Liu, Y., 2012. Geotextile tube dewatering of contaminated sediments, Tianjin Eco-City, China. Geotext. Geomembranes 31, 39–50.
Yuan, J., Feng, W.Z., Jiang, X.M., Wang, J.L., 2019. Saline-alkali migration in soda saline soil based on sub-soiling technology. Desalination Water Treat. 149, 352–362.
Zhan, C., de Jong, M., de Bruijn, H., 2018. Funding sustainable cities: a comparative study of Sino-Singapore Tianjin eco-city and Shenzhen international low-carbon city. Sustainability 10, 4256.
Zhang, X.G., Huang, B., Liu, F., 2020. Information extraction and dynamic evaluation of soil salinization with a remote sensing method in a typical county on the Huang-Huai-Hai Plain of China. Pedosphere 2020 30, 496–507.
Zhu, G.R., Xu, X.G., Wang, H., Li, T.Y., Feng, Z., 2017. The ecological cost of land reclamation and its enlightenment to coast sustainable development in the northwestern Bohai Bay, China. Acta Oceanol. Sin. 36, 97–104.
Zou, Y.L., Hu, F.L., Zhou, C.C., Li, C.L., Dunn, K.J., 2013. Analysis of radial basis function interpolation approach. Appl. Geophys. 10, 397–410.